Innovative x-ray measurement diagnostic for impurity transport study on ITER

D. Colette[1]*, D. Mazon[1], R. Barnsley[2], M. O'Mullane[3], A. Jardin[4], A. Sirinelli[2], M. Walsh[2]

[1] CEA, IRFM, F-13108 Saint Paul Lez Durance, France
[2] ITER Organization, Route de Vinon sur Verdon, 13067 St Paul Lez Durance Cedex, France
[3] Departments of Physics SUPA, University of Strathclyde, Glasgow, G4 ONG, UK
[4] Institute of Nuclear Physics Polish Academy of Sciences (IFJ PAN), PL-31-342, Krakow, Poland

1 Introduction

In tokamaks with Tungsten plasma facing components such as ITER, pollution of the plasma by heavy impurities is a major concern. Indeed, the x-ray radiation emitted by such impurities (mostly in the [0.1, 100] keV range) deteriorates the reactor performance and can even lead to radiative breakdown. X-ray tomography is a key diagnostics for impurity transport studies and can also be used to detect instabilities and measure electron temperature, provided that the measurement is spectrally-resolved. Because of the harsh radiation environment on ITER during its nuclear phase, advanced detectors exhibiting high resilience to neutrons and *gamma* rays such as gas filled detectors are required. The use of the Low Voltage Ionization Chamber (LVIC) has been proposed in [1] and is investigated in this work. The tomographic capabilities of the LVIC are first studied. The measurement volume of the LVIC is divided thanks to the addition of anodes in order to allow spectral deconvolution of the x-ray emissivity. This innovative modification and an associated inversion method are presented and applied to the computation of the electron temperature profile on ITER.

2 Low Voltage Ionization Chamber synthetic diagnostic

A LVIC is a gas-filled x-ray detector which converts incident photons into electron-ion pairs by photoelectric effect. An electric field is applied between two electrodes in order to capture the generated electron cloud on the anode, leading to the collection of an electrical current which can be measured. The LVIC therefore operates in current mode, which does not allow the extraction of any spectral information. Due to a small inter-electrodes distance, the LVIC can be operated at a low voltage which allows its power supply to be located far from the detector and limits radiation damage to the system.
Modelling of the LVIC is achieved by computing the transmission through filters (e.g. beryllium window or detector casing) using cross-sections from the NIST XCOM database. [2]. The photoionization of the gas is computed for argon or xenon using cross-sections from the NIST XCOM database. [2], and takes into account the Fano noise (i.e. the statistical fluctuation of the size of the electron cloud). The deexcitation of the ionized atom of gas is simulated by considering the competition between Auger emission and x-ray fluorescence. The photon emitted through x-ray fluorescence is considered to escape the detection volume without interacting with the gas. The electric field in the chamber is considered to be high enough so that all

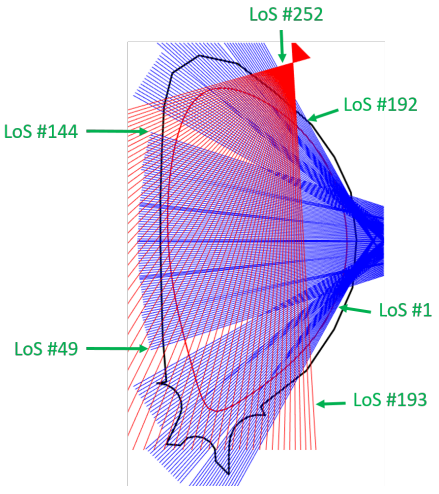

Figure 1: *Geometry of the radial x-ray cameras lines-of-sight (blue) and added vertical lines-of-sight (red).*

*Corresponding author : damien.colette@iter.org

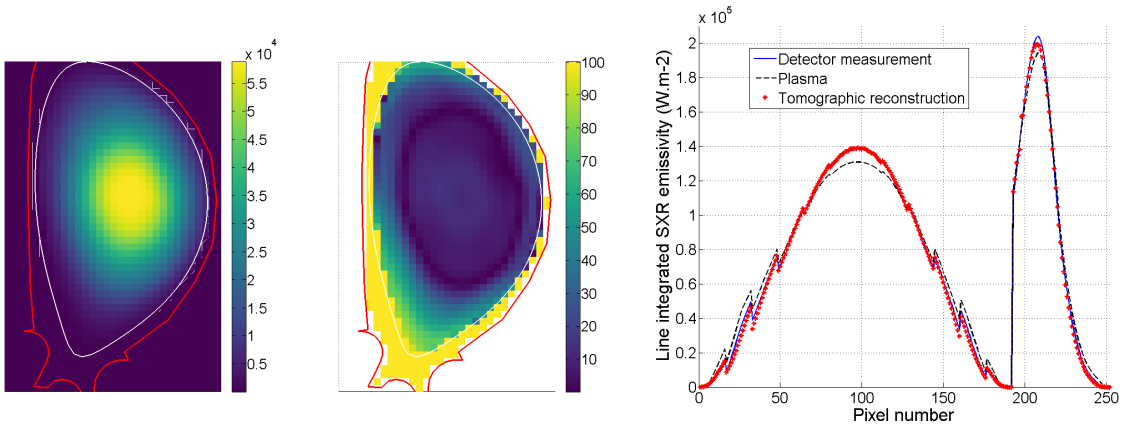

Figure 2: Left: Reconstructed emissivity profile ($W \cdot m^{-}3$). Center: Reconstruction error (%). Right: LVIC measurement, line-integrated emissivity, and its reconstruction ($W \cdot m^{-2}$).

the electrons are collected on the anode. The modelled current is calibrated in order to reconstruct the surface-integrated incoming x-ray power on the detector over an energy range which depends on the LVIC parameters (e.g. gas, depth, pressure). More details on the simulation of the LVIC can be found in [3].
The synthetic diagnostic is coupled to a Minimum Fisher Information algorithm [4] in order to reconstruct the 2D x-ray emissivity profile. The geometry of the ITER x-ray cameras lines-of-sight is shown in blue on fig. 1. It has been demonstrated in [3] that these lines-of-sight do not allow the reconstruction of asymmetric emissivity profiles and as a result "vertical" lines-of-sight (in red) are added in this study. The reconstructed emissivity profile in the [0, 50] keV energy range obtained using a xenon-filled LVIC with a depth of 150 mm and a pressure of 1 bar is shown on fig. 2. A good agreement between the emissivity and its reconstruction can be seen in the plasma core. The error obtained in the line-integrated emissivity comes from the calibration method and could be corrected with energy-resolved measurement (see [3]).

3 Multi-anodes LVIC and energy discrimination

In order to perform spectral deconvolution of the x-ray flux impinging the detector, the detection volume of the LVIC is divided into sub-chambers through the addition of anodes (see fig. 3). This division leads to a shift of the spectral response towards higher energies from a sub-chamber to the next, as shown on fig. 4.

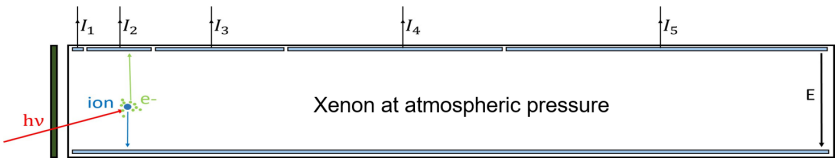

Figure 3: *Schematics of a multi-anodes LVIC (MA-LVIC).*

The currents measured by each sub-chamber can be coupled using an inversion method in order to deconvolute the spectrum. This inversion is a so-called ill-posed problem, and it therefore requires a priori information on the x-ray spectrum either through regularization or a hypothesis on the spectrum shape. The latter option is used in this work and, based on our knowledge on x-ray emissivity in plasmas, a simple mathematical function can be defined in order to fit the x-ray spectrum. The function models two emissivity peaks (located at 2 and 7 keV) and the exponential decrease of the flux at high energy, and is expressed as:

$$f(h\nu \geq 10) = X_1 \cdot e^{-X_2 \cdot h\nu} \cdot C_{cor}(h\nu)$$

$$f(h\nu < 10) = X_3 \cdot e^{-2\cdot(h\nu-7)^2} + X_4 \cdot e^{-1.5\cdot(h\nu-2)^2} + \frac{X_1 \cdot e^{-X_2 \cdot 10}}{10} \cdot h\nu$$

A gradient descent-based algorithm is used to find the quadruplet $X = (X_1, X_2, X_3, X_4)$ which leads to reconstructed sub-chamber currents as close as possible to those which were obtained through simulation. This is achieved by minimizing $r(X) = \Sigma(I^{simu} - I^{rec}(X))^2$.

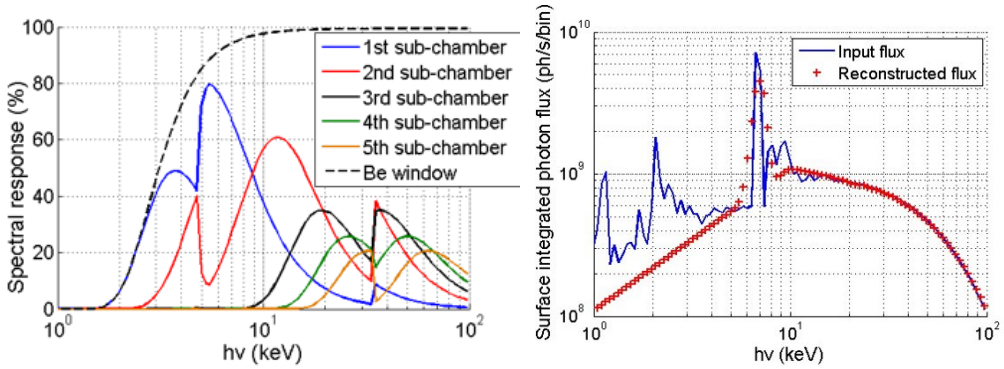

Figure 4: *Left: Spectral response of the different sub-chambers of a MA-LVIC. Right: Energy deconvolution of the photon flux impinging channel number 96 (looking at the plasma core). The MA-LVIC is filled with xenon at atmospheric pressure, with anode sizes of 5, 30, 60, 100, and 150 mm and a* $200\mu m$ *deep beryllium window.*

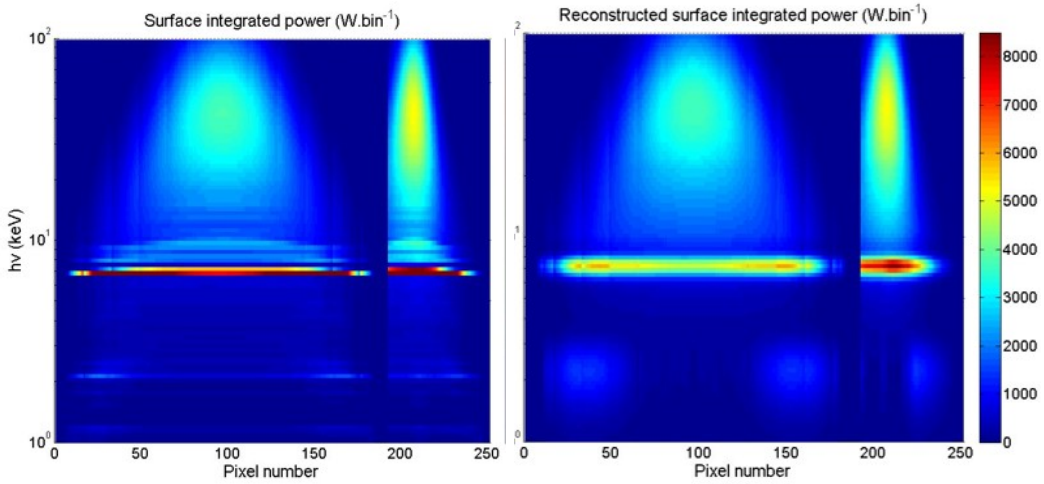

Figure 5: Reconstruction of the x-ray emissivity spectrum.

The results of spectral deconvolution using this method and for a radial line-of-sight looking at the plasma core are displayed on fig. 4. It can be observed that the continuum part of the spectrum ($h\nu \geq 10keV$) is very accurately reconstructed. The height of peak located around 7 keV is not reproduced accurately but as the reconstructed peak is wider, the peak integral is well reconstructed. The peak around 2 keV is not reconstructed at all ($X_3 = 0$), which is explained by the lack of information at low energy because of the beryllium window. [5]
The conclusions of this single line-of-sight analysis are confirmed when considering all the x-ray cameras lines-of-sight (shown on fig. 5): there is a very good reconstruction of the continuum part of the spectrum and the 7 keV peak (in terms of integral), but there is a lack of accuracy at low energy. The profiles of surface integrated power in each energy bin can be coupled to a tomographic algorithm in order to obtain spectrally-resolved 2D emissivity profiles. This is carried on using the Minimum Fisher Information algorithm [4] which was used in the previous section. The results are shown in fig. 6 for a pixel at the very core of the plasma. It can be observed the both the 7 keV peak and the continuous part of the spectrum are accurately reconstructed.

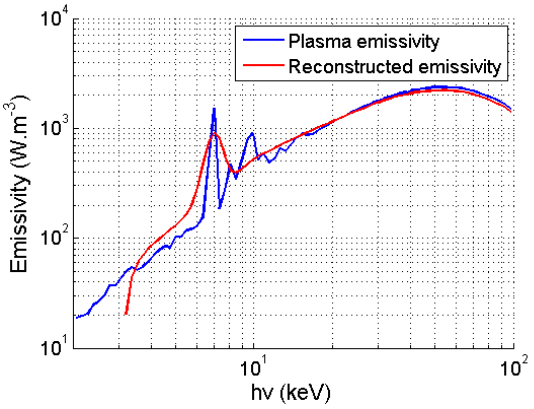

Figure 6: *Reconstruction of the local plasma emissivity in the plasma core.*

4 Electron temperature reconstruction

The shape of the continuous x-ray spectrum mostly depends on the local electron temperature profile [6]. As a result, an accurate reconstruction of the high energy part of the spectrum allows the reconstruction of the electron temperature. In this work, the slope of the exponential decrease is computed for every pixel of the plasma cross-section and the electron temperature is extracted from it. The results are presented in fig. 7, the reconstruction is accurate at the very core of the plasma.

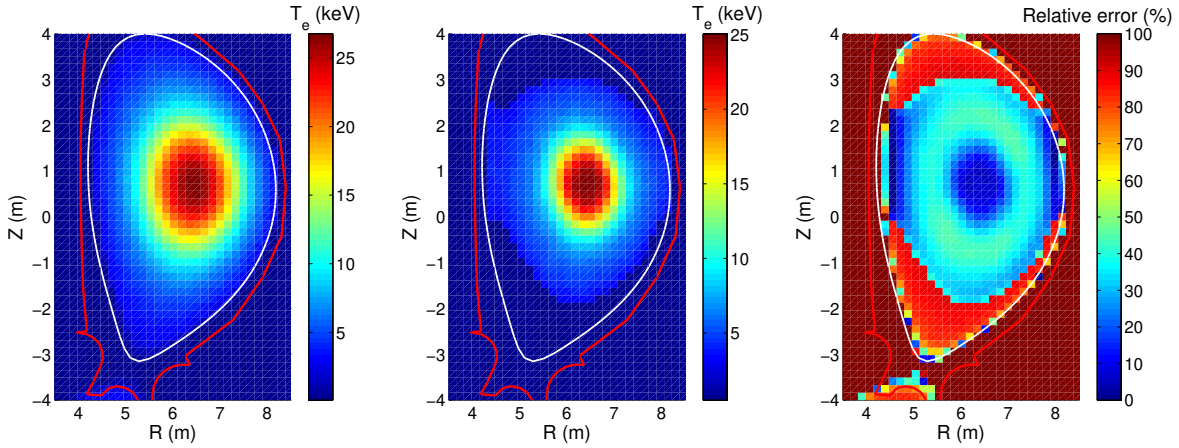

Figure 7: *Left: Electron temperature profile of the ITER standard high power D-T scenario. Center: Reconstructed electron temperature profile obtained after energy resolved tomography. Right: Relative reconstruction error of the electron temperature (%).*

5 Conclusions and perspectives

This work shows that the LVIC is a very good radiation hard candidate for x-ray measurement on ITER. It indeed allows an accurate tomographic reconstruction of the emissivity with spectral resolution over a fairly wide energy range. Additional parameters such as the electron temperature can be extracted from the energy-resolved measurement. Improvements can be achieved by performing simultaneous spectral and spatial deconvolution, allowing regularization in both spaces at once. Experimental validation of the model used to simulate the LVIC measurement process can be achieved through experimental testing of a LVIC prototype, which is currently ongoing.

6 Acknowledgements

The authors would like to thank Dr. Christian Ingesson for his valuable inputs. We would like to thank our Chinese Colleagues from ASIPP for their fruitful inputs, especially regarding the input geometry for the Diagnostic First Wall (DFW) apertures and in-plug slits. This work was supported by the ITER Organisation through the SSA72. The views and opinions expressed in this paper do not necessarily reflect those of the ITER Organisation nor those of Fusion for Energy.

References

[1] Y. V. Gott et al, A low-voltage ionization chamber for the ITER, M.M. Instrum Exp Tech 52: 260, 2009

[2] M.J. Berger et al, XCOM: Photon cross sections database, NIST Standard Reference Database, 8, 87-3597, 2009

[3] D. Colette et al, Modeling a low voltage ionization chamber based tomography system on ITER, Rev. Sci. Instrum. 91, 2020

[4] D. Mazon et al, Soft x-ray tomography for real-time applications: Present status at Tore Supra and possible future developments, The Review of scientific instruments, 83, 063505, 10.1063/1.4730044, 2012

[5] D. Colette, Innovative x-ray diagnostic for impurity transport on ITER, Aix-Marseille Université, 2021

[6] G. H. McCall, Calculation of X-ray bremsstrahlung and characteristic line emission produced by a Maxwellian electron distribution, Journal of Physics D: Applied Physics, 1982, https://doi.org/10.1088/0022-3727/15/5/012